JOURNAL OF CATALYSIS **141**, 161–170 (1993)

Calcination-Induced Surface Enrichment of Impurities and Its Effect on Catalytic Properties of Iron Oxide

B. L. YANG,[1] S. B. LEE, D. S. CHENG, AND W. S. CHANG

National Central University, Chemical Engineering Department, Chung-Li, Taiwan, Republic of China

Received September 23, 1992; revised December 21, 1992

The possible role of surface heterogeneities as activity sources on α-Fe_2O_3 was studied by high-temperature calcination, which resulted in surface smoothing and selective enrichment of impurities at the surface. Among the six impurities, Ca, Mn, Mg, Zn, Ni, and Si, found in the bulk of a commercial α-Fe_2O_3 (99.9%), only Si and Ca were enriched at the surface after high-temperature calcination. Silicon contamination at the surface (up to about 30% surface cation composition) had little effect on the catalytic performance of iron oxide in butene oxidative dehydrogenation. Calcium, on the other hand, showed a strong poisoning effect on both the dehydrogenation and the combustion site, thus served as a probe in locating the active sites on α-Fe_2O_3. Washing the high-temperature-calcined sample with water or nitric acid resulted in the removal of surface calcium and the restoration of the activity. Based on a high-magnification SEM comparison between a just-calcined and a water-washed sample, it was suggested that the active sites on α-Fe_2O_3 are located at the surface steps. © 1993 Academic Press, Inc.

INTRODUCTION

It is always of interest to understand the nature and location of an active site on a catalyst surface. In a series of reports on the study of iron oxide and ferrite catalysts in the oxidative dehydrogenation of butene, two kinds of active sites, the dehydrogenation site and the combustion site, have been found (*1–7*). The active sites on different iron oxides have very different properties. For example, butene adsorbed at the dehydrogenation site on α-Fe_2O_3 is easily degraded by gaseous oxygen (*2*), while that on γ-Fe_2O_3 is not (*3*). Although the atomic structure of the active site has yet to be identified, the densities of the active site (number of sites per unit surface area) have been measured (*1–3*). For those iron oxide and ferrite catalysts studied, all measurements suggest that the active sites represent no more than a few percent of the cation population at the surface.

The low density of active sites on iron oxide catalysts has prompted several postulates for the nature and the location of the active sites. One postulate that the active site is associated with surface adsorbed oxygen was found to be incorrect (*2*). Other possibilities involve surface defects or heterogeneities, or the presence of foreign elements.

The involvement of defects in heterogeneous catalysis has long been proposed. Sleight and Linn (*8*) reported a strong correlation between the activity of a Pb–Bi–Mo–O catalyst and its bulk concentration of cation vacancies. Surface science studies on metal single crystals have shown that surfaces of different crystal planes have different catalytic properties and step surfaces of high indices often pose higher catalytic activities than low-index flat surfaces (*9, 10*).

One simple way to study the possible relationship between active site and surface de-

---

[1] To whom correspondence should be addressed at Northwestern University, Chemical Engineering Department, Evanston, IL 60208.

0021-9517/93 $5.00

fect is high-temperature calcination, which usually results in sintering of the oxide and the reduction of surface heterogeneity. Thus by comparing catalysts calcined at different temperatures, one can gain some understanding about the role of surface heterogeneity. If the active sites are constituted of foreign elements or point defects induced by impurities, some insight of the active site can be obtained by monitoring the impurity at the surface. High-temperature treatment may promote surface enrichment of impurities.

We report in this paper the results of such a high-temperature calcination study on α-Fe_2O_3. It was found that calcium and silicon were enriched at the surface of α-Fe_2O_3 after high-temperature calcination. While calcium exhibited a strong poisoning effect, silicon appeared to have little impact on the catalytic properties of iron oxide. Based on the results of a high-magnification scanning electron microscopy (SEM) study coupled with selective surface calcium removal, it is suggested that the active sites for butene oxidation are located at surface steps on α-Fe_2O_3.

EXPERIMENTAL

Reagent grade (99.9%) and high-purity (99.999%, Puratronic) α-Fe_2O_3 were purchased from Alfa Chemicals. Air calcination was performed at 600, 800, or 1000°C for 24 hr either using an uncovered porcelain crucible or a covered platinum crucible. Some calcined samples were washed with nitric acid (2 *N*) at room temperature followed by repeated wash with doubly distilled water (DDW), or washed only with DDW.

X-Ray photoelectron spectroscopy (XPS) was performed on a VG Microlab MK-III spectrometer with a spherical sector analyzer operated in the constant pass energy (50 eV) mode. Al$K\alpha$ X-ray (1486.6 eV) was used for the excitation. The oxide powder was pressed onto a piece of indium foil (99.999%), which was grounded to the spectrometer during spectra collection. No electron flood gun was used. Surface cation compositions were calculated using the sensitivity factors provided by the manufacturer. The sensitivity factors are 5.43, 0.855, and 5.13 for Fe $2p_{1/2}$, Si $2s$, and Ca $2p$, respectively. To calculate molar composition, peak areas are divided by their individual sensitivity factors.

High-magnification SEM was performed on cold field-emission electron microscopes Hitachi S-800 and ABT DS-130F. Low electron acceleration voltages (5 to 8 kV) were used to allow rich imaging of surface feature. The samples were coated with Pt or Pt–Pd before examination. Other characterizations included nitrogen volumetric adsorption for BET surface area measurement, X-ray diffraction (XRD) for crystal phase identification, and inductively coupled plasma atomic emission spectroscopy (ICP-AES) for bulk impurity analysis. For ICP-AES, iron oxide powders were first dissolved in hydrochloric acid (Merck, 32%). Special care was taken in silicon analysis, for the hydrochloric acid used had a measurable silicon contamination by itself.

The performance of the catalysts in butene oxidative dehydrogenation was studied both in pulse and flow reaction mode. The apparatus and the procedure have been reported elsewhere (*2*, *11*). For pulse reactions, the amounts of catalysts used were adjusted to keep a constant total surface area of 0.5 m^2. The catalyst was first purged with helium at 300°C for 1 hr and at 500°C for 5 min to remove adsorbed CO_2 and H_2O. The pulse reactions were conducted in the absence of gaseous oxygen.

The densities of active sites were measured by using an adsorption–desorption technique developed earlier (*1*, *2*). The procedure started with the same purge–clean pretreatment of the catalyst as for pulse reaction. The catalyst was then equilibrated with 1-butene at -78°C, followed by a thorough purge with helium at the same temperature. After that, thermal desorption was performed and the desorbed butadiene, CO_2, and 2-butene isomers were quantified

TABLE 1

BET Surface Area, Crystallite Size, and Flow Reaction Performance[a] of α-Fe_2O_3 (99.9%) Calcined at Different Temperatures

Calc. temp.[b] (°C)	Wash cond.	Cryst. size (μm)	BET area (m^2/g)	Amnt. used (g)	Rxn. temp. (°C)	1-C_4H_8 conv.[c] (%)	C_4H_6 sel.[c] (%)
600	—	<0.1	6.6	0.10	350	9	62
800	—	0.3	2.0	0.34	350	4	60
					400	30	58
1000	—	1.0	0.28	0.80	350	0	—
					400	0	—
					450	4	34
1000	H_2O 6 hr	1.0	0.28	0.80	400	10	63

[a] Flow rates He : 1-C_4H_8 : O_2 = 58 : 2 : 2 ml/min.

[b] In uncovered porcelain crucible in air for 24 hr.

[c] Steady-state values: conv = $(C_4H_6 + CO_2/4)/(C_4H_8 + C_4H_6 + CO_2/4)$; sel = $C_4H_6/(C_4H_6 + CO_2/4)$.

to give the dehydrogenation, the combustion, and the isomerization site density, respectively. Control experiments were done to confirm the fulfillment of the basic requirements for active site density measurements: (i) saturation of active sites with butene, (ii) no readsorption of desorbed products, and (iii) each site adsorbs only one butene.

RESULTS

X-ray diffraction results revealed that all iron oxide catalysts studied in this work were α-Fe_2O_3. Table 1 gives the BET surface areas, representative crystallite sizes (SEM data), and steady-state reaction performance of some α-Fe_2O_3 (99.9%) samples after different calcination treatments. A decrease in activity with the increase in calcination temperature is clearly observed. Washing the 1000°C-calcined α-Fe_2O_3 (99.9%) with water restored some of its activity.

XPS was employed to study the possible surface contamination caused by high temperature calcination. After a careful search, only two contaminants, Si and Ca, were detected. Their surface concentrations as a function of calcination condition and posttreatment are given in Table 2. To determine the source of contamination, a batch of α-Fe_2O_3 (99.9%) was calcined in a covered platinum crucible instead of an uncovered porcelain crucible. After calcination at 1000°C for 24 hr, the α-Fe_2O_3 in platinum crucible had about the same level of calcium contamination on the surface but had only about two-thirds of the silicon contamination as that found on the sample calcined in a porcelain crucible. This suggests that calcium was originated from the bulk of α-Fe_2O_3 and was enriched at the surface due to high temperature air calcination, while silicon came from both the bulk of α-Fe_2O_3 and the porcelain crucible. The impurities in α-Fe_2O_3 (99.9%) bulk, as analyzed by ICP-AES, are given in Table 3.

The high-purity α-Fe_2O_3 (99.999%) showed no detectable surface contamination after 1000°C calcination in a covered platinum crucible. After it was calcined in a porcelain crucible, the sample was contaminated by silicon but not calcium, indicating again that a porcelain crucible, when used at high temperatures, is a source of silicon contamination.

If the 1000°C-calcined α-Fe_2O_3 (99.9%) was washed with water (DDW), one-third of the surface calcium was removed (Table

TABLE 2

Surface Contamination of Calcined α-Fe_2O_3 as Monitored by XPS

Catalyst	Calc. temp.[a] (°C)	Crucible used[b]	Wash cond.	Surface cation comp. (mole%)		
				Fe	Si	Ca
α-Fe_2O_3 (99.9%)	600	U.P.	—	98	2	0
	800	U.P.	—	97	3	0
	1000	U.P.	—	56	32	12
			H_2O 6 hr	63	29	8
			HNO_3 1 hr	78	22	0
	1000	C.Pt	—	68	20	12
α-Fe_2O_3 (99.999%)	1000	U.P.	—	75	25	0
	1000	C.Pt	—	100	0	0

[a] 24 hr in air.

[b] U.P. = uncovered porcelain crucible; C.Pt = covered platinum crucible.

2). Washing with 2 *N* nitric acid removed surface calcium completely, but had only a limited effect on silicon removal. There were no measurable BET surface area changes after either wash.

Pulse reaction of 1-butene over differently calcined and washed α-Fe_2O_3 was studied and the results are given in Table 4. Little carbon dioxide was produced because most combustion sites on α-Fe_2O_3 are not active at 300°C. The high CO_2 yields observed in the flow reaction at comparable temperatures were mainly resulted from the degradation of butadiene precursors on the dehydrogenation sites by gaseous oxygen (*2*, *3*). As can be seen in Table 4, high-temperature calcination resulted in a decrease of activity for α-Fe_2O_3 (99.9%), in agreement with flow reaction data (Table 1). Water and nitric acid wash helped to restore the activity of the contaminated α-Fe_2O_3 (99.9%), but has little effect on the high-purity α-Fe_2O_3 (99.999%).

TABLE 3

Impurities in α-Fe_2O_3 (99.9%) as Measured by ICP-AES

Impurity	Bulk atomic ratio[a] M/Fe
Ca	0.00048
Mn	0.00031
Mg	0.00022
Zn	0.000094
Ni	0.000089
Si	0.000062

[a] M = impurity element.

Several points can be noted here: (1) Washing with nitric acid for 10 or 1 hr had the same effect, suggesting that the effect of acid wash was complete within 1 hr (based on catalytic evaluation). (2) Compared with nitric acid wash, water wash restored about half of activity of the 1000°C calcined α-Fe_2O_3 (99.9%). (3) The nitric acid wash had little effect on the least contaminated 600°C-calcined α-Fe_2O_3 (99.9%) and on the silicon-contaminated but calcium-free α-Fe_2O_3 (99.999%). This indicates that nitric acid wash does not alter the catalytic properties of a clean α-Fe_2O_3 surface. (4) After nitric acid wash, the 600-, 800-, and 1000°C-calcined α-Fe_2O_3 (99.9%) showed comparable activities. (5) The catalytic activty of α-Fe_2O_3 was found to strongly depend on calcium contamination at its surface, but not on silicon contamination.

TABLE 4

Pulse Reaction of 1-Butene at 300°C over Differently Calcined and Washed α-Fe_2O_3[a]

Catalyst	Calc. temp. (°C)	Wash cond.	Product yield (%)			
			C_4H_6	$CO_2/4$	t-2-C_4H_8	c-2-C_4H_8
α-Fe_2O_3 (99.9%)	600	—	19.5	0.2	8.0	8.7
		HNO_3 1 hr	22.4	0.4	10.0	10.3
	800	—	15.7	0	6.6	7.4
		H_2O 6 hr	20.7	0.2	18.7	18.2
		HNO_3 1 hr	22.7	0.2	20.6	19.9
	1000	—	0	0	0	0
		H_2O 6 hr	11.5	0	9.6	11.7
		HNO_3 1 hr	23.3	0	21.4	20.6
		HNO_3 10 hr	22.4	0	19.3	20.0
α-Fe_2O_3[b] (99.999%)	1000	—	7.2	0	5.2	6.5
		H_2O 12 hr	9.1	0	6.5	8.2
		HNO_3 1 hr	8.1	0	7.7	9.8

[a] Pulse size 4.3 × 10^{-6} mole 1-butene in helium (30 ml/min) with no gaseous oxygen. Amount of catalyst adjusted to maintain a constant surface area of 0.5 m^2 except footnote b.

[b] BET surface area not measured, 0.5 g of catalyst used for each run.

Table 5 gives the active site densities of some selected samples of α-Fe_2O_3 (99.9%). The numbers paralleled the pulse reaction data in Table 4, showing the loss of active sites by high-temperature calcination and their recovery by water and nitric acid wash.

Figure 1 gives the SEM pictures of the 1000°C-calcined α-Fe_2O_3 (99.9%) before and after water wash. At the first glance, the just-calcined α-Fe_2O_3 sample appeared to be neat, while the washed sampled showed breakage of some agglomerates and the presence of small debris. When surface features were examined carefully at high magnifications, fine differences became visible. While the just-calcined α-Fe_2O_3 (99.9%) showed a smooth and featureless surface, the washed sample exhibited a pattern of circular stripes on its surface. When a lower acceleration voltage (5 kV) was used, the difference between the two samples became even more visible (Fig. 2), although some degradation of the picture quality resulted. The same pattern was also seen on the nitric-acid-washed samples.

Since calcium oxide is soluble in water

TABLE 5

Active Site Densities on Some α-Fe_2O_3 (99.9%) Samples

Calc. temp.[a] (°C)	Wash cond.	Site density ($10^{17}/m^2$)		
		Dehydrogenation	Combustion	Isomerization
600	—	1.5	1.1	1.6
800	—	0.9	0.6	0.9
1000	—	0	0	0
	H_2O 6 hr	0.6	1.0	1.8
	HNO_3 1 hr	1.8	1.4	2.7

[a] Calcined in a porcelain crucible in air for 24 hr.

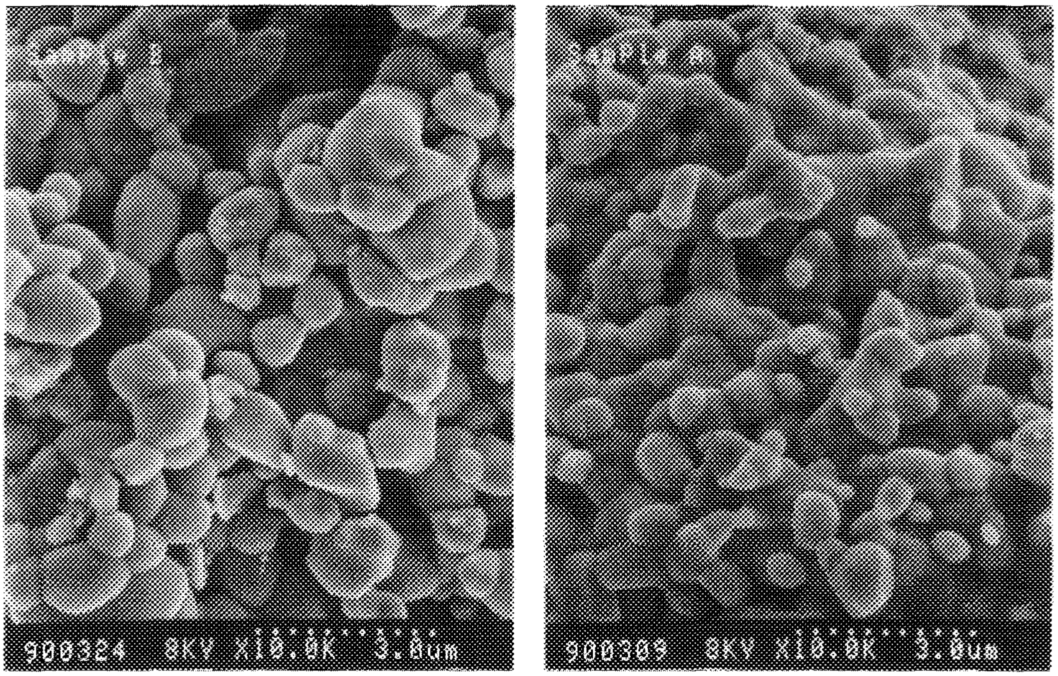

FIG. 1. SEM pictures of the 1000°C calcined α-Fe_2O_3 (99.9%) before and after water wash. Samples coated with Pt: (A) before wash; (B) after wash.

while iron oxide is practically insoluble, it is likely that the stripes observed in SEM of the washed sample were resulted from calcium dissolution. To confirm this, 10 g of 1000°C-calcined α-Fe_2O_3 (99.9%) was soaked in 10 ml of DDW for 6 hr. The water was then collected for ICP-AES analysis of calcium and iron. Indeed, the water was found rich in calcium with little iron, having a Ca/Fe atomic ratio of 37. This confirms the selective removal of calcium by DDW. We have thus observed both the reexposure of surface steps and the restoration of catalytic activity of the 1000°C-calcined α-Fe_2O_3 by surface calcium removal.

Soaking 10 g of 1000°C-calcined α-Fe_2O_3 (99.9%) in 10 ml of 2 *N* nitric acid for 1 hr gave a Ca/Fe atomic ratio of 1.5, indicating still the preferential dissolution of calcium over iron in nitric acid. Based on the fact that no surface calcium was detected by XPS after nitric acid wash, it can be estimated from ICP-AES results that 40% of calcium in the α-Fe_2O_3 (99.9%) had segregated from the bulk to the surface after 1000°C calcination for 24 hr.

DISCUSSION

Surface enrichment in alloys (*12*) and in ceramic materials (*13, 14*) has been studied extensively and has found important engineering applications. The enrichment in alloys is determined by the minimization of surface free energy, or surface tension, such that the component having the lowest surface tension tends to be most enriched at the surface (*12*). The enrichment in ceramic materials appears to be more complicated. It depends on the nature of the matrix, the properties of the enriching component, and the gaseous environment the solid is exposed to (*14–16*). Surface enrichment can be very important to oxide catalysts also, because calcination is commonly the final step in oxide catalyst preparation, and the

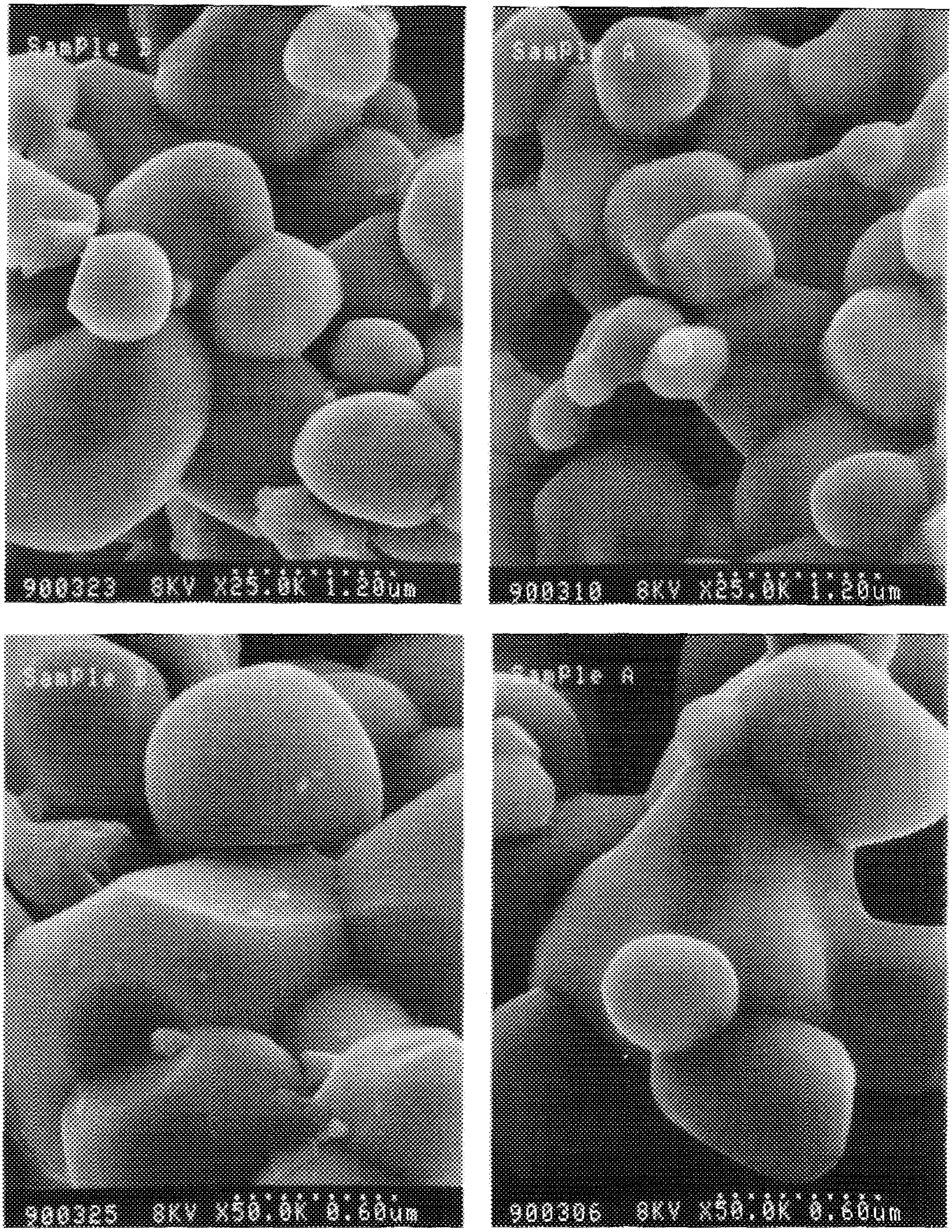

FIG. 1—*Continued*

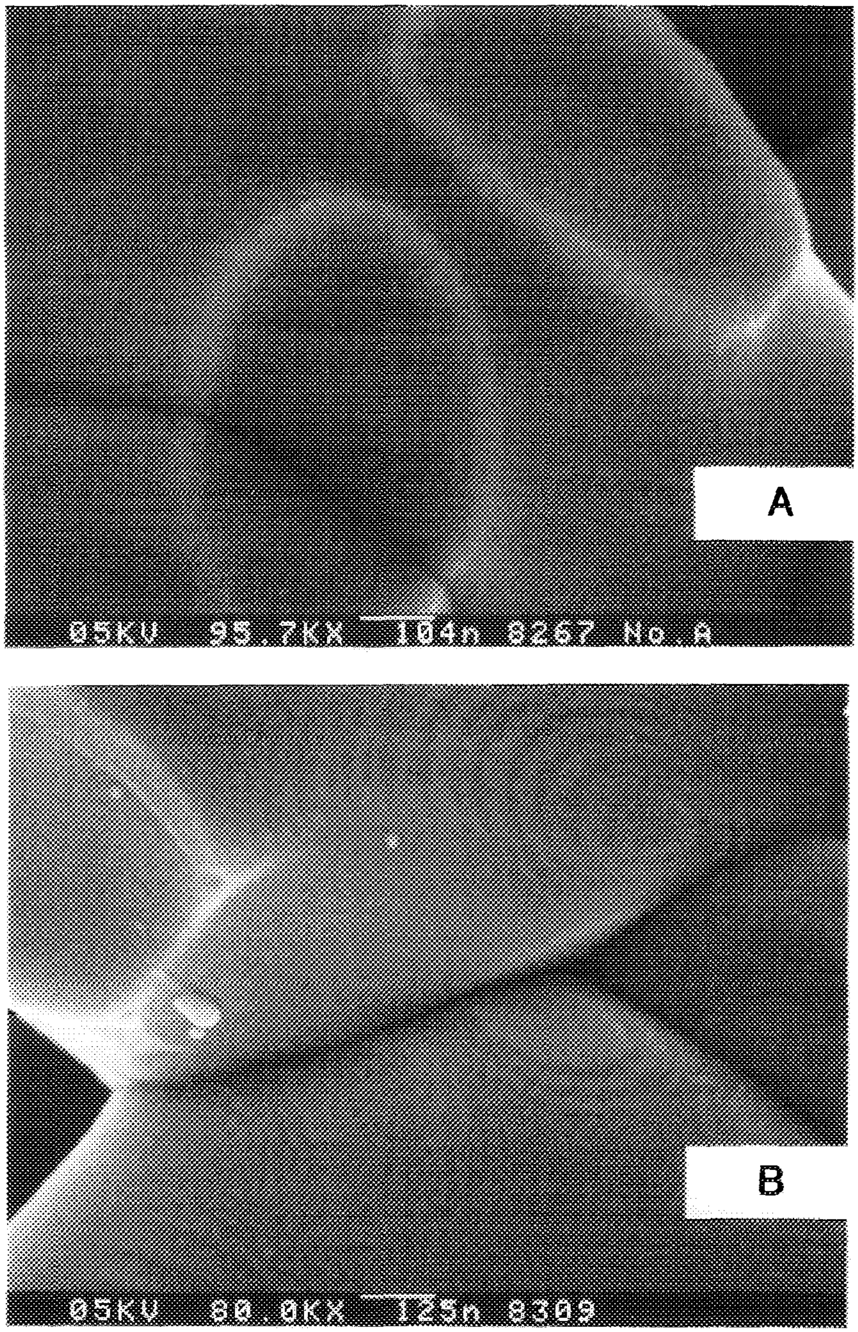

FIG. 2. High magnification SEM pictures of the 1000°C calcined α-Fe_2O_3 (99.9%) obtained at 5 kV. Samples coated with Pt–Pd: (A) before wash; (B) after water wash.

high temperature employed can promote the enrichment.

Tables 2 and 3 demonstrate clearly that surface enrichment of impurities in α-Fe_2O_3 is highly selective. Out of the six detectable impurities in the bulk of α-Fe_2O_3, only Ca and Si are enriched at the surface during air calcination at high temperatures. The other four elements that remain in the bulk, Mg, Mn, Zn, and Ni, share a common character of being able to form spinel ferrites with iron oxide. It is possible that this chemical affinity helps keep them in the bulk. The enrichment factors for Si and Ca at 1000°C can be calculated to be 3000 and 250, respectively. XPS results indicate that both silicon and calcium are in the oxidized states, but do not allow further identification of their chemical forms. However, since the enrichment factors for Si and Ca are so great, it is not likely that stoichiometric iron silicate or calcium ferrite are the segregated phases at the surface. Rather, silicon oxide and calcium oxide/carbonate are the more probable forms.

On the nature of the active site, there is no evidence that the oxidative dehydrogenation activity of iron oxide could be originated from foreign elements. For the two elements that were enriched at the surface, silicon showed little effect on the catalytic performance of iron oxide, while calcium showed a strong poisoning effect.

The mechanism by which calcium poisons an active site is unclear. Calcium could physically block an active site, or change the chemistry of an active site by reacting with it, or form calcium carbonate close enough to an active site to hinder its access. But in any case, calcium segregated from the bulk must have been driven selectively to the active site or its close vicinity. The calcium can thus serve as a probe in locating the active sites at the surface, should we have the capability of chemical differentiation at an atomic resolution. However, neither EPMA nor SIMS mapping had sufficient lateral resolution to locate the calcium at the surface.

Combining high-magnification SEM and ICP-AES results, it is suggested that calcium removal from the surface resulted in the reexposure of surface steps. As can be seen in Fig. 2, these steps are 20 to 60 nm wide, probably also tens of nm high. Although they are about 10 times wider and taller than those commonly generated on single crystal surfaces, it is logical to assume that they still share the basic features of surface steps, such as a high degree of coordinative unsaturation for atoms at the step edge. Coordinative unsaturation is generally considered essential for the initiation of reactant–catalyst interaction. Since calcium removal also resulted in the restoration of the activity, it is very likely that the active sites on iron oxide are located at surface steps. This speculation is in accordance with the fact that the active sites on α-Fe_2O_3 represent only a few percent of surface cations.

Although we can not exclude the possibility that a small fraction of calcium could be well dispersed on the flat surface of α-Fe_2O_3 and its removal was SEM invisible, it is difficult to attribute the poisoning effect to such a small fraction of surface calcium. If each active site is poisoned by one calcium atom, it can be estimated that only 11% of the surface calcium as measured by ICP-AES on the 1000°C-calcined α-Fe_2O_3 (99.9%) was needed to poison all the active sites. One would then anticipate a highly nonlinear relationship between the removal of calcium and the restoration of the activity. This is, however, not observed. The fact that calcium removal resulted in a surface morphology change strong enough to permit SEM differentiation also suggests that calcium tends to aggregate instead of disperse at the surface of iron oxide.

While the active sites are selectively poisoned by calcium but not by silicon, the calcium does not appear to discriminate its attack on the three kinds of active site, the dehydrogenation, the combustion, and the isomerization site. Tables 4 and 5 show parallel losses of dehydrogenation and isomerization activity due to calcium contamination, and parallel regeneration of the three active sites by removing surface calcium. The fact that calcium does not discriminate the three active sites indicates the presence of a common feature among the three sites. It is possible that the three sites share the same geometric feature, like the surface step suggested by SEM, but are different in local structure or chemistry. Further work is needed to probe and differentiate the three active sites.

The inertness of surface silicon is interesting. Although silicon oxide has long been used as a binding material for industrial catalysts and has generally been considered to be catalytically inert, it was reported to have a strong promoting effect on iron oxide for the oxidative dehydrogenation of butene (*17*). By coprecipitating 5% silica into iron oxide, Iizuka *et al.* (*17*) observed a 2.3 times increase in butadiene formation rate per unit surface area. The surface composition of this silica added iron oxide was not reported, but it would be logical to assume that some silica may have appeared at the surface. The promoting effect was attributed by those authors to extra surface acidity induced by silicon incorporated into the iron oxide lattice. However, the fact that surface silicon appeared to be inert in this study suggests that the promoting effect observed by Iizuka *et al.* could be much more complicated. It is also possible that the addition of silicon oxide to iron oxide resulted in structural defects and surface heterogeneities, which contributed to the high activity. Indeed, by adding 5% silica into iron oxide, Iizuka *et al.* found that the resulted mixed oxide was X-ray amorphous (*17*).

ACKNOWLEDGMENTS

The authors express their appreciation to Professor Harold H. Kung at Northwestern University for his long-term inspiration and encouragement. The National Science Council of the Republic of China is acknowledged for financially supporting this work. The authors also thank Mr. Shean-Ren Horng and Miss Rita Hwang of Industrial Technology Research Institute, Hsinchu, Taiwan, for collecting XPS data, and the ABT Corp. for providing some low-kV SEM pictures.

REFERENCES

1. Kung, M. C., Cheng, W. H., and Kung, H. H., *J. Phys. Chem.* **83,** 1737 (1979).
2. Yang, B. L., and Kung, H. H., *J. Catal.* **77,** 410 (1982).
3. Yang, B. L., Kung, M. C., and Kung, H. H., *J. Catal.* **89,** 172 (1984).
4. Liaw, B. J., Cheng, D. S., Yang, S. J., and Yang, B. L., *J. Chin. Chem. Soc.* **37,** 463 (1990).
5. Kung, H. H., and Kung, M. C., *in* "Advances in Catalysis," (D. D. Eley, H. Pines and P. B. Weisz Eds.), Vol. 33, pp. 159–198, Academic Press, Orlando, Florida, 1985.
6. Kung, H. H., Kundalkar, B., Kung, M. C., and Cheng, W. H., *J. Phys. Chem.* **84,** 382 (1980).
7. Yang, B. L., Cheng, D. S., and Lee, S. B., *Appl. Catal.* **70,** 161 (1991).
8. Sleight, A. W., and Linn, W. J., *Ann. N. Y. Acad. Sci.* **272,** 22 (1976).
9. Somorjai, G. A., "Chemistry in Two Dimensions: Surfaces." Cornell Univ. Press, Ithaca, New York, 1981.
10. Strongin, D. R., and Somorjai, G. A., *J. Catal.* **118,** 99 (1989).
11. Liaw, B. J., Cheng, D. S., and Yang, B. L., *J. Catal.* **118,** 312 (1989).
12. Kuczynski, G. C., and Carberry, J. J., *Chem. Phys. Lett.* **111,** 445 (1984).
13. Levinson, L. M. (Ed.), "Grain Boundary Phenomena in Electronic Ceramics," Advances in Ceramics, Vol. 1. Am. Ceram. Soc., Columbus, Ohio, 1981.
14. Nowotny, J., and Dufour, L. C. (Eds.), "Surface and Near-Surface Chemistry of Oxide Materials." Elsevier, Amsterdam, 1988.
15. Kingery, W. D., *Pure Appl. Chem.* **56,** 1703 (1984).
16. Yang, B. L., Chan, S. F., Chang, W. S., and Chen, Y. Z., *J. Catal.* **130,** 52 (1991).
17. Iizuka, T., Tatsumi, H., and Tanabe, K., *Aust. J. Chem.* **35,** 919 (1982).